Available online at www.sciencedirect.com
SCIENCE DIRECT®
ELSEVIER
International Journal of Solids and Structures 41 (2004) 6197–6214
INTERNATIONAL JOURNAL OF SOLIDS and STRUCTURES
www.elsevier.com/locate/ijsolstr

Transient analysis of a mode-III crack propagating in a piezoelectric medium

Yi-Shyong Ing *, Mau-Jung Wang

Department of Aerospace Engineering, Tamkang University, 151 Ying-chuan Road, Tamsui, Taipei 251, Taiwan, ROC

Received 7 March 2004; received in revised form 6 May 2004
Available online 10 June 2004

Abstract

The transient response of a semi-infinite, propagating crack subjected to dynamic anti-plane concentrated loading in a piezoelectric medium is investigated. A new fundamental solution for the piezoelectric material is proposed and the transient response of the propagating crack is determined by superposition of the fundamental solution in the Laplace transform domain. Exact analytical transient solutions for the dynamic stress intensity factor, the dynamic electric displacement intensity factor, and the dynamic energy release rate are obtained by using the Cagniard method of Laplace inversion and are expressed in explicit forms. The results indicate that the dynamic intensities of a propagating crack can be represented by the product of a universal function and the corresponding solution for a stationary crack. It is also found that the dynamic stress intensity factor and the dynamic energy release rate go to zero as the propagating speed approaches the Bleustein–Gulyaev piezoelectric surface wave speed under this particular boundary condition.

Keywords: Propagating crack; Piezoelectric material; Dynamic fracture; Surface wave

1. Introduction

This work is a continuation of the study given by Ing and Wang (2004) in which the attention was focused on the investigation of transient responses of a stationary crack subjected to anti-plane loading in a piezoelectric material. In this study, a further investigation is performed to understand dynamic fracture responses of a propagating piezoelectric crack subjected to a pair of concentrated loadings on crack faces. The transient behavior of a piezoelectric crack from stationary to propagation is analyzed and discussed in detail.

Recently, due to the intrinsic electro-mechanical coupling behaviors, piezoelectric materials have been widely used as actuating and sensing devices in smart structures. Because of the brittle properties of most piezoelectric materials, the failure analysis of piezoelectric structures has attracted more attention from many researchers. Most of studies, however, are related to static or quasi-static conditions, e.g. Pak (1990), Sosa (1992), Suo et al. (1992), Park and Sun (1995a,b), Zhang and Tong (1996), Narita and Shindo (1998a),

* Corresponding author. Tel.: +886-2-26215656x2617; fax: +886-2-26209746.
E-mail address: ysing@mail.tku.edu.tw (Y.-S. Ing).

0020-7683/$ - see front matter © 2004 Elsevier Ltd. All rights reserved.
doi:10.1016/j.ijsolstr.2004.05.019

Qin and Mai (1998), Gao and Fan (1999a,b), Shen et al. (1999), Yang and Kao (1999), Kwon and Lee (2000), Ru (2000), Gao and Wang (2001), Yang (2001), and Li (2003). Because of the mathematical complications, less attention has been paid to the study of dynamic fracture mechanics of piezoelectric materials. Shindo and Ozawa (1990) first investigated the steady-state response of a cracked piezoelectric material subjected to plane harmonic waves. Afterward the dynamic fracture analysis of piezoelectric materials was developed rapidly. For example, the single crack problem had been investigated by Chen (1998), Narita and Shindo (1998b, 1999), Chen and Karihaloo (1999), Li (2001), Kwon and Lee (2001), Shin et al. (2001), Meguid and Zhao (2002), and Ueda (2003), while the multiple cracks problem had been studied by Wang and Meguid (2000), Wang et al. (2000), Meguid and Chen (2001), Wang (2001), Zhao and Meguid (2002), and Zhou et al. (2003). However, due to the mathematical difficulties, most of the researchers obtained their solutions by means of some numerical methods. The exact analytical solutions for cracked piezoelectric materials are rare.

In the study of crack propagation, Yoffe (1951) was the first one to investigate a steady-state crack growth problem of a crack of fixed length propagating in an infinite and purely elastic body subjected to a uniform remote tensile stress. Subsequently, many researchers were devoted to the study of crack propagation for purely elastic solids, e.g. Kostrov (1964, 1966), Achenbach (1970a,b), Freund (1972a,b, 1973, 1974), Ma and Burgers (1986, 1987, 1988), and Ma (1988, 1990). For piezoelectric crack problems, Li and Mataga (1996a,b) first obtained transient closed-form solutions for dynamic stress and electric displacement intensities and dynamic energy release rate of a propagating crack in hexagonal piezoelectric materials. They assumed that the crack surfaces are electrode- or vacuum-type boundary conditions and the dynamic anti-plane point loading is initially applied at the stationary crack tip. Hence there is no characteristic length presented in their problems. Chen and Yu (1997) studied the problem of anti-plane Yoffe's crack in an unbounded piezoelectric medium. Later, Chen et al. (1998) investigated the response of a finite Griffith crack propagating along the interface of two dissimilar piezoelectric half-planes. Recently, Kwon et al. (2000) investigated the crack problem of an infinitely long piezoelectric ceramic strip containing a Griffith crack moving with constant velocity.

In this study, the transient response of a semi-infinite propagating crack subjected to dynamic anti-plane concentrated loading on the crack faces in a hexagonal piezoelectric medium is investigated. The inherent characteristic length makes the problem more difficult. A new fundamental solution is derived and the transient solution is determined by superposition of the fundamental solution in the Laplace transform domain. Similar superposition techniques had been successfully used to solve many transient problems of a stationary crack (Ing and Ma, 1996, 1997a, 2001, submitted for publication; Ing and Wang, 2004) and a propagating crack (Ing and Ma, 1997b, 1999, 2003; Ing and Lin, 2002) for purely elastic solids. It demonstrates a powerful method to deal with crack problems with characteristic lengths. Under the assumption of electrode boundary condition on crack surfaces (Bleustein, 1968; Li and Mataga, 1996a), exact analytical transient solutions for the dynamic stress intensity factor, the dynamic electric displacement intensity factor, and the dynamic energy release rate are obtained. Although the metallic coating condition is chiefly a mathematically convenient proposition, this boundary condition is also appropriate if the crack surfaces are in a state of electric contact, or if the crack is filled with conducting gas or liquid (Li and Mataga, 1996a). Only the intensities and energy release rate are derived in this study, however, the transient full-field solutions for the crack propagation problem can also be obtained by using the fundamental solutions proposed in the study.

2. Fundamental solutions of distributed loads applied on propagating crack faces

In this section, a fundamental problem is proposed and the associated fundamental solutions will be used to solve the complicated problem of a propagating crack with a characteristic length in the next section.

Consider an unbounded hexagonal piezoelectric medium containing a semi-infinite crack that lies on the negative ξ-axis and propagates with a constant velocity v along the crack tip line. It is assumed that the propagating crack surfaces are perfectly covered with an infinitesimally thin conducting electrode that is grounded, such that the electrostatic potential vanishes over the entire crack surfaces. The solutions for an anti-plane exponentially distributed traction applied to the propagating crack faces in the Laplace transform domain will be referred to as the fundamental solutions. Because of the anti-symmetry of the problem, it can be viewed as a half-plane problem with material occupying the region of $y \geqslant 0$, and subjected to the following mixed boundary conditions in the Laplace transform domain

$$\overline{\tau}_{yz}(\xi, 0, s) = \mathrm{e}^{s\eta\xi}, \quad \text{for } -\infty < \xi < 0, \tag{1}$$

$$\overline{\phi}(\xi, 0, s) = 0, \quad \text{for } -\infty < \xi < \infty, \tag{2}$$

$$\overline{w}(\xi, 0, s) = 0, \quad \text{for } 0 < \xi < \infty, \tag{3}$$

where s is the Laplace transform parameter, and η is a constant. The coordinate ξ is fixed with respect to the moving crack tip. The overbar symbol is used for denoting the transform on time t. The one-sided Laplace transform with respect to time and the two-sided Laplace transform with respect to ξ are defined by (Achenbach, 1973)

$$\overline{f}(\xi, y, s) = \int_0^\infty f(\xi, y, t)\,\mathrm{e}^{-st}\,\mathrm{d}t, \tag{4}$$

$$\overline{f}^*(\lambda, y, s) = \int_{-\infty}^\infty \overline{f}(\xi, y, s)\,\mathrm{e}^{-s\lambda\xi}\,\mathrm{d}\xi. \tag{5}$$

If we consider only the out-of-plane displacement and the in-plane electric fields, the dynamic anti-plane governing equations for a hexagonal piezoelectric material (6 mm) can be described in the fixed coordinate system x–y by

$$c_{44}\nabla^2 w + e_{15}\nabla^2\phi = \rho\ddot{w}, \tag{6}$$

$$e_{15}\nabla^2 w - \varepsilon_{11}\nabla^2\phi = 0, \tag{7}$$

where $w = w(x, y, t)$ is the anti-plane displacement in the z-direction (which is assumed to aligned with the hexagonal symmetry axis), $\phi = \phi(x, y, t)$ is the electric potential, c_{44} is the elastic modulus measured in a constant electric field, ε_{11} is the dielectric permittivity measured at a constant strain, e_{15} is the piezoelectric constant, and ρ is the material density. $\nabla^2 = \partial^2/\partial x^2 + \partial^2/\partial y^2$ is the in-plane Laplacian and a dot denotes material time derivative.

The constitutive equations for the piezoelectric material can be expressed as

$$\tau_{xz} = c_{44}\frac{\partial w}{\partial x} + e_{15}\frac{\partial\phi}{\partial x}, \tag{8}$$

$$\tau_{yz} = c_{44}\frac{\partial w}{\partial y} + e_{15}\frac{\partial\phi}{\partial y}, \tag{9}$$

$$D_x = e_{15}\frac{\partial w}{\partial x} - \varepsilon_{11}\frac{\partial\phi}{\partial x}, \tag{10}$$

$$D_y = e_{15}\frac{\partial w}{\partial y} - \varepsilon_{11}\frac{\partial\phi}{\partial y}, \tag{11}$$

where τ_{xz} and τ_{yz} are the shear stress components, and D_x and D_y are the electric displacements.

In analyzing this problem, it is convenient to express the relevant equations in the moving coordinates ξ–y. Setting $\xi = x - vt$ and making use of the transformation proposed by Bleustein (1968), the governing and constitutive equations may be rewritten as follows

$$(1 - b^2v^2)\frac{\partial^2 w}{\partial \xi^2} + \frac{\partial^2 w}{\partial y^2} + 2b^2 v \frac{\partial^2 w}{\partial \xi \, \partial t} - b^2 \frac{\partial^2 w}{\partial t^2} = 0, \tag{12}$$

$$\frac{\partial^2 \psi}{\partial \xi^2} + \frac{\partial^2 \psi}{\partial y^2} = 0, \tag{13}$$

$$\tau_{\xi z} = \overline{c}_{44} \frac{\partial w}{\partial \xi} + e_{15} \frac{\partial \psi}{\partial \xi} \tag{14}$$

$$\tau_{yz} = \overline{c}_{44} \frac{\partial w}{\partial y} + e_{15} \frac{\partial \psi}{\partial y}, \tag{15}$$

$$D_{\xi} = -\varepsilon_{11} \frac{\partial \psi}{\partial \xi}, \tag{16}$$

$$D_{y} = -\varepsilon_{11} \frac{\partial \psi}{\partial y}, \tag{17}$$

where

$$\psi = \phi - \frac{e_{15}}{\varepsilon_{11}} w \tag{18}$$

and

$$\overline{c}_{44} = c_{44} + \frac{e_{15}^2}{\varepsilon_{11}} \tag{19}$$

is the piezoelectrically stiffened elastic constant.

To solve the fundamental problem with the governing equations (12) and (13) and the mixed-type boundary conditions (1)–(3), the integral transform method and the Wiener–Hopf technique will be implemented in the following derivation. From (12) and (13), the general solutions for $\overline{w}^*$ and $\overline{\psi}^*$ (in the upper half-plane $y \geqslant 0$) in the double transformed domain can be obtained as follows

$$\overline{w}^*(\lambda, y, s) = A(s, \lambda) \, \mathrm{e}^{-s\alpha^*(\lambda) y}, \tag{20}$$

$$\overline{\psi}^*(\lambda, y, s) = B(s, \lambda) \, \mathrm{e}^{-s\beta^*(\lambda) y}, \tag{21}$$

where

$$\alpha^*(\lambda) = \sqrt{b^2 - 2b^2 v\lambda + b^2 v^2 \lambda^2 - \lambda^2}, \tag{22}$$

$$\beta^*(\lambda) = \lim_{\varepsilon \to 0} \sqrt{\varepsilon^2 - \lambda^2}, \tag{23}$$

and

$$b = \frac{1}{c} = \sqrt{\frac{\rho}{\overline{c}_{44}}}$$

is the slowness of the bulk shear wave in the piezoelectric material. $\varepsilon \to 0^+$ is an auxiliary positive real perturbation parameter (Li and Mataga, 1996a,b).

Application of the two-sided Laplace transform to (1)–(3) yields

$$\overline{\tau}^*_{yz}(\lambda, 0, s) = \frac{1}{s(\eta - \lambda)} + \overline{\tau}^*_+(\lambda, s), \tag{24}$$

$$\overline{\phi}^*(\lambda, 0, s) = 0, \tag{25}$$

$$\overline{w}^*(\lambda, 0, s) = \overline{w}^*_-(\lambda, s), \tag{26}$$

where $Re(\eta) > Re(\lambda)$. The unknown function τ_+ is defined to be the shear stress τ_{yz} on the plane $y = 0$ for $0 < \xi < \infty$. Likewise, w_- is defined to be the displacement in the z-direction of the crack face $y = 0^+$ for $-\infty < \xi < 0$. From (18) and (25), we will have $B(s, \lambda) = -e_{15}A(s, \lambda)/\varepsilon_{11}$. Substitution of (20) into (26) leads to $A = \overline{w}^*_-$. Then making use of (15) and substituting it into the transformed stress boundary condition (24), we can have the following Wiener–Hopf equation

$$-\overline{c}_{44}[\alpha^*(\lambda) - k_e^2\beta^*(\lambda)]\overline{w}^*_-(\lambda, s) = \frac{1}{s^2(\eta - \lambda)} + \frac{\overline{\tau}^*_+(\lambda, s)}{s}, \tag{27}$$

where

$$k_e = \sqrt{\frac{e_{15}^2}{\overline{c}_{44}\varepsilon_{11}}} \tag{28}$$

is the electro-mechanical coupling coefficient for the electrode boundary condition. It is noted that the bracketed term $\alpha^*(\lambda) - k_e^2\beta^*(\lambda)$ in the left-hand side of (27) corresponds to the Bleustein–Gulyaev wave function (Bleustein, 1968).

At this point it is convenient to introduce a new function $S^*(\lambda)$ by defining

$$S^*(\lambda) = \frac{\alpha^*(\lambda) - k_e^2\beta^*(\lambda)}{(\sqrt{1 - b^2v^2} - k_e^2)\sqrt{1/(c_{\mathrm{bg}} - v) + \lambda}\sqrt{1/(c_{\mathrm{bg}} + v) - \lambda}}, \tag{29}$$

where

$$c_{\mathrm{bg}} = \sqrt{\frac{\overline{c}_{44}(1 - k_e^4)}{\rho}} \tag{30}$$

is the Bleustein–Gulyaev piezoelectric surface wave speed shielded with electrode. It is assumed in this study that the crack speed v does not exceed c_{bg}. Under this assumption, the function $S^*(\lambda)$ has the properties that $S^*(\lambda) \to 1$ as $|\lambda| \to \infty$, and $S^*(\lambda)$ has neither zeros nor poles in the λ-plane by cuts along $-1/(c_{\mathrm{bg}} - v) < \lambda < -\varepsilon$ and $\varepsilon < \lambda < 1/(c_{\mathrm{bg}} + v)$. From the general product factorization method, $S^*(\lambda)$ can be written as the product of two regular functions $S^*_+(\lambda)$ and $S^*_-(\lambda)$, where

$$S^*_+(\lambda) = \sqrt{\frac{1/(c_{\mathrm{bg}} - v) + \lambda}{1/(c - v) + \lambda}}Q^*_+(\lambda) \tag{31}$$

and

$$S^*_-(\lambda) = \sqrt{\frac{1/(c_{\mathrm{bg}} + v) - \lambda}{1/(c + v) - \lambda}}Q^*_-(\lambda) \tag{32}$$

in which

$$Q_+^*(\lambda) = \exp\left\{\frac{1}{\pi}\int_{\varepsilon}^{\frac{1}{c-v}} \tan^{-1}\left[\frac{k_e^2 z}{\alpha^*(-z)}\right]\frac{\mathrm{d}z}{z+\lambda}\right\}, \tag{33}$$

$$Q_-^*(\lambda) = \exp\left\{\frac{1}{\pi}\int_{\varepsilon}^{\frac{1}{c+v}} \tan^{-1}\left[\frac{k_e^2 z}{\alpha^*(z)}\right]\frac{\mathrm{d}z}{z-\lambda}\right\}. \tag{34}$$

In view of the previous discussion, Eq. (27) may be rewritten as

$$-\overline{c}_{44}(\sqrt{1-b^2v^2}-k_e^2)\frac{1/(c_{\mathrm{bg}}+v)-\lambda}{\sqrt{1/(c+v)-\lambda}}Q_-^*(\lambda)\overline{w}_-^*(\lambda,s) = \frac{M_+^*(\lambda)}{s^2(\eta-\lambda)} - \frac{M_+^*(\lambda)\overline{\tau}_+^*(\lambda,s)}{s}, \tag{35}$$

where

$$M_+^*(\lambda) = \frac{\sqrt{1/(c-v)+\lambda}}{[1/(c_{\mathrm{bg}}-v)+\lambda]Q_+^*(\lambda)}. \tag{36}$$

The first term on the right-hand side is regular for $Re(\lambda) > -\varepsilon$, except for the pole at $\lambda = \eta$. This pole can, however, be removed by writing

$$\frac{M_+^*(\lambda)}{s^2(\eta-\lambda)} = \frac{M_+^*(\lambda)-M_+^*(\eta)}{s^2(\eta-\lambda)} + \frac{M_+^*(\eta)}{s^2(\eta-\lambda)}. \tag{37}$$

Eq. (35) can now be rearranged into the desired form

$$\begin{aligned}&-\overline{c}_{44}(\sqrt{1-b^2v^2}-k_e^2)\frac{1/(c_{\mathrm{bg}}+v)-\lambda}{\sqrt{1/(c+v)-\lambda}}Q_-^*(\lambda)\overline{w}_-^*(\lambda,s) - \frac{M_+^*(\eta)}{s^2(\eta-\lambda)}\\ &\quad = \frac{M_+^*(\lambda)-M_+^*(\eta)}{s^2(\eta-\lambda)} + \frac{M_+^*(\lambda)\overline{\tau}_+^*(\lambda,s)}{s}.\end{aligned} \tag{38}$$

The left-hand side of this equation is regular for $Re(\lambda) < 0$, while the right-hand side is regular for $Re(\lambda) > -\varepsilon$. Applying the analytic continuation argument, therefore, each side of (38) represents a single entire function, say $E(\lambda)$. By Liouville's theorem, the bounded entire function $E(\lambda)$ is a constant. The magnitude of the constant can be obtained from order conditions on $E(\lambda)$ as $|\lambda| \to \infty$, which in turn are obtained from order conditions on the dependent field variables in the vicinity of $\xi = 0$. Furthermore, $\overline{\tau}_+(\xi,0,s)$ is expected to be square root singular near $\xi = 0$, i.e. $\overline{\tau}_+(\xi,0,s) = \mathrm{O}(|\xi|^{-1/2})$ as $\xi \to 0^+$. By using of the Abelian theorem, $E(\lambda)$ vanishes identically, and then we can solve for $\overline{w}_-^*$ from the left-hand side of (38). Since the amplitude of displacement $A(s,\lambda) = \overline{w}_-^*$ in the Laplace transform domain, we find

$$A(s,\lambda) = -\frac{M_+^*(\eta)\sqrt{1/(c+v)-\lambda}}{\overline{c}_{44}(\sqrt{1-b^2v^2}-k_e^2)s^2(\eta-\lambda)[1/(c_{\mathrm{bg}}+v)-\lambda]Q_-^*(\lambda)}. \tag{39}$$

Then the amplitude of $\overline{\psi}^*$ can be obtained as follows

$$B(s,\lambda) = -\frac{e_{15}}{\varepsilon_{11}}A(s,\lambda) = \frac{k_e^2 M_+^*(\eta)\sqrt{1/(c+v)-\lambda}}{e_{15}(\sqrt{1-b^2v^2}-k_e^2)s^2(\eta-\lambda)[1/(c_{bg}+v)-\lambda]Q_-^*(\lambda)}. \tag{40}$$

Substituting (39) and (40) into (20) and (21) and making use of (18) and (14)–(17), and then inverting the two-sided Laplace transform, we can obtain solutions for the fundamental problem in the Laplace transform domain as follows

$$\overline{w}(\xi,y,s)=\frac{-1}{2\pi \mathrm{i}}\int_{\Gamma_\lambda}\frac{M_+^*(\eta)\sqrt{1/(c+v)-\lambda}}{\overline{c}_{44}(\sqrt{1-b^2v^2}-k_e^2)s(\eta-\lambda)[1/(c_{\mathrm{bg}}+v)-\lambda]Q_-^*(\lambda)}\mathrm{e}^{-s\alpha^*(\lambda)y+s\lambda\xi}\,\mathrm{d}\lambda, \tag{41}$$

$$\begin{aligned}\overline{\phi}(\xi,y,s)=&\frac{-1}{2\pi \mathrm{i}}\int_{\Gamma_\lambda}\frac{k_e^2M_+^*(\eta)\sqrt{1/(c+v)-\lambda}}{e_{15}(\sqrt{1-b^2v^2}-k_e^2)s(\eta-\lambda)[1/(c_{\mathrm{bg}}+v)-\lambda]Q_-^*(\lambda)}\mathrm{e}^{-s\alpha^*(\lambda)y+s\lambda\xi}\,\mathrm{d}\lambda\\&+\frac{1}{2\pi \mathrm{i}}\int_{\Gamma_\lambda}\frac{k_e^2M_+^*(\eta)\sqrt{1/(c+v)-\lambda}}{e_{15}(\sqrt{1-b^2v^2}-k_e^2)s(\eta-\lambda)[1/(c_{\mathrm{bg}}+v)-\lambda]Q_-^*(\lambda)}\mathrm{e}^{-s\beta^*(\lambda)y+s\lambda\xi}\,\mathrm{d}\lambda,\end{aligned} \tag{42}$$

$$\begin{aligned}\overline{\tau}_{\xi z}(\xi,y,s)=&\frac{-1}{2\pi \mathrm{i}}\int_{\Gamma_\lambda}\frac{M_+^*(\eta)\lambda\sqrt{1/(c+v)-\lambda}}{(\sqrt{1-b^2v^2}-k_e^2)(\eta-\lambda)[1/(c_{\mathrm{bg}}+v)-\lambda]Q_-^*(\lambda)}\mathrm{e}^{-s\alpha^*(\lambda)y+s\lambda\xi}\,\mathrm{d}\lambda\\&+\frac{1}{2\pi \mathrm{i}}\int_{\Gamma_\lambda}\frac{k_e^2M_+^*(\eta)\lambda\sqrt{1/(c+v)-\lambda}}{(\sqrt{1-b^2v^2}-k_e^2)(\eta-\lambda)[1/(c_{\mathrm{bg}}+v)-\lambda]Q_-^*(\lambda)}\mathrm{e}^{-s\beta^*(\lambda)y+s\lambda\xi}\,\mathrm{d}\lambda,\end{aligned} \tag{43}$$

$$\begin{aligned}\overline{\tau}_{yz}(\xi,y,s)=&\frac{1}{2\pi \mathrm{i}}\int_{\Gamma_\lambda}\frac{M_+^*(\eta)\alpha^*(\lambda)\sqrt{1/(c+v)-\lambda}}{(\sqrt{1-b^2v^2}-k_e^2)(\eta-\lambda)[1/(c_{\mathrm{bg}}+v)-\lambda]Q_-^*(\lambda)}\mathrm{e}^{-s\alpha^*(\lambda)y+s\lambda\xi}\,\mathrm{d}\lambda\\&-\frac{1}{2\pi \mathrm{i}}\int_{\Gamma_\lambda}\frac{k_e^2M_+^*(\eta)\alpha^*(\lambda)\sqrt{1/(c+v)-\lambda}}{(\sqrt{1-b^2v^2}-k_e^2)(\eta-\lambda)[1/(c_{\mathrm{bg}}+v)-\lambda]Q_-^*(\lambda)}\mathrm{e}^{-s\beta^*(\lambda)y+s\lambda\xi}\,\mathrm{d}\lambda,\end{aligned} \tag{44}$$

$$\overline{D}_\xi(\xi,y,s)=-\frac{1}{2\pi \mathrm{i}}\int_{\Gamma_\lambda}\frac{\varepsilon_{11}k_e^2M_+^*(\eta)\lambda\sqrt{1/(c+v)-\lambda}}{e_{15}(\sqrt{1-b^2v^2}-k_e^2)(\eta-\lambda)[1/(c_{\mathrm{bg}}+v)-\lambda]Q_-^*(\lambda)}\mathrm{e}^{-s\beta^*(\lambda)y+s\lambda\xi}\,\mathrm{d}\lambda, \tag{45}$$

$$\overline{D}_y(\xi,y,s)=\frac{1}{2\pi \mathrm{i}}\int_{\Gamma_\lambda}\frac{\varepsilon_{11}k_e^2M_+^*(\eta)\beta^*(\lambda)\sqrt{1/(c+v)-\lambda}}{e_{15}(\sqrt{1-b^2v^2}-k_e^2)(\eta-\lambda)[1/(c_{\mathrm{bg}}+v)-\lambda]Q_-^*(\lambda)}\mathrm{e}^{-s\beta^*(\lambda)y+s\lambda\xi}\,\mathrm{d}\lambda. \tag{46}$$

The corresponding results of the dynamic stress intensity factor and the dynamic electric displacement intensity factor expressed in the Laplace transform domain are

$$\overline{K}_{\mathrm{III}}^{(\tau)}(s)=\lim_{\xi\to0}\sqrt{2\pi\xi}\overline{\tau}_{yz}(\xi,0,s)=-\frac{\sqrt{2}M_+^*(\eta)}{\sqrt{s}} \tag{47}$$

and

$$\overline{K}_{\mathrm{III}}^{(D)}(s)=\lim_{\xi\to0}\sqrt{2\pi\xi}\overline{D}_y(\xi,0,s)=-\frac{\varepsilon_{11}k_e^2\sqrt{2}M_+^*(\eta)}{e_{15}(\sqrt{1-b^2v^2}-k_e^2)\sqrt{s}}, \tag{48}$$

respectively.

3. Transient analysis of a propagating crack in a piezoelectric medium

Consider a semi-infinite crack located at $y=0$, $x<0$ in an unbounded hexagonal piezoelectric medium as shown in Fig. 1. It is assumed that the crack surfaces are completely coated with an infinitesimally thin perfectly conducting electrode that is grounded, such that the electrostatic potential vanishes over the crack surfaces. For time $t<0$, the piezoelectric medium is stress free and at rest. At time $t=0$, a pair of equal and opposite dynamic anti-plane concentrated loadings with magnitude p are applied at the crack faces with a

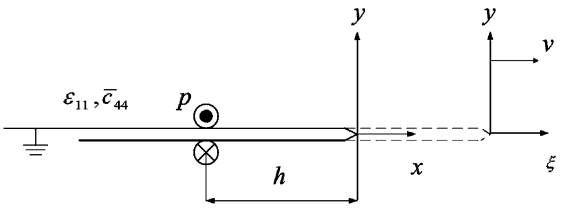

Fig. 1. Configuration and coordinate systems of a propagating crack in a piezoelectric medium.

distance h from the crack tip. The time dependence of the concentrated loading is represented by the Heaviside function $H(t)$. The boundary condition for the applied loading can be represented by

$$\tau_{yz}(x,0,t) = -p\delta(x+h)H(t) \tag{49}$$

where $\delta(\ )$ is the Dirac delta function. The incident field of the cylindrical wave generated by the concentrated loading expressed in the Laplace transform domain can be obtained as follows

$$\overline{\tau}_{yz}(x,0,s) = \frac{1}{2\pi \mathrm{i}} \int_{\Gamma_\lambda} -p\, \mathrm{e}^{s\lambda(h+x)}\, \mathrm{d}\lambda. \tag{50}$$

The applied traction on the crack faces as indicated in (50), has the functional form $\mathrm{e}^{s\lambda x}$. Since the solutions of applying traction $\mathrm{e}^{s\eta x}$ on crack faces have been solved in Section 2 (by setting $v = 0$), the diffracted field generated from the crack tip can be constructed by superimposing the incident wave traction that is equal to (50). Because the dynamic stress and electric displacement intensities and the dynamic energy release rate are the key parameters in characterizing dynamic crack growth, we will focus our attention mainly on the determination of these quantities. When we combine (47) and (50) (by setting $v = 0$), the dynamic stress intensity factor expressed in the Laplace transform domain can be obtained as follows

$$\overline{K}_{\mathrm{III}}^{(\tau),s}(s) = \frac{1}{2\pi \mathrm{i}} \int_{\Gamma_\lambda} -p\, \mathrm{e}^{s\lambda h} \left\{ -\frac{\sqrt{2} M_+(\lambda)}{\sqrt{s}} \right\} \mathrm{d}\lambda, \tag{51}$$

where

$$M_+(\lambda) = M_+^*(\lambda)\big|_{v=0} = \frac{\sqrt{b+\lambda}}{(b_{\mathrm{bg}}+\lambda) Q_+(\lambda)}. \tag{52}$$

In Eq. (52), $Q_+(\lambda) = Q_+^*(\lambda)\big|_{v=0}$ and $b_{\mathrm{bg}} = 1/c_{\mathrm{bg}}$ is the slowness of the Bleustein–Gulyaev piezoelectric surface wave for the electrode boundary. By using the Cagniard method (Cagniard, 1939) of Laplace inversion, the dynamic stress intensity factor of the stationary crack in time domain can be obtained as follows

$$K_{\mathrm{III}}^{(\tau),s}(t) = \sqrt{\frac{2}{\pi^3 h}} p \int_0^t Re\left[\frac{\sqrt{\tau - bh}}{\sqrt{t-\tau}(\tau - b_{\mathrm{bg}}h) Q_+(-\tau/h)} \right] \mathrm{d}\tau\, H(b_{\mathrm{bg}}h - t) + p\sqrt{\frac{2}{\pi h}} H(t - b_{\mathrm{bg}}h). \tag{53}$$

It is noticed that the bracketed term in the integrand of (53) is a purely imaginary number as $t < bh$, so $K_{\mathrm{III}}^{(\tau),s}(t)$ equals zero before the shear wave arrives at the crack tip. The reason is that for the particular case of the electrode boundary condition considered here, the electrostatic potential is zero along the entire line $y = 0$. Consequently, there is no effect from electric field to the dynamic intensity factor before the incident shear wave is diffracted by the crack tip. It can be found that (53) has a pole singularity at $\tau = b_{\mathrm{bg}}h$, which corresponds to the instant of arrival of the Bleustein–Gulyaev piezoelectric surface wave. Moreover, the

magnitude of the dynamic stress intensity factor jumps from infinity to the appropriate static value ($p\sqrt{2/(\pi h)}$) right after the Bleustein–Gulyaev surface wave passes through the crack tip. This result is similar to that of purely elastic solids.

Similarly, combining (48) and (50) (by setting $v = 0$), the dynamic electric displacement intensity factor can be represented in the Laplace transform domain as follows

$$\overline{K}_{\mathrm{III}}^{(D),s}(s) = \frac{1}{2\pi \mathrm{i}} \int_{\Gamma_\lambda} -p \mathrm{e}^{s\lambda h} \left\{ -\frac{\varepsilon_{11} k_e^2 \sqrt{2} M_+(\lambda)}{e_{15}(1-k_e^2)\sqrt{s}} \right\} \mathrm{d}\lambda. \tag{54}$$

Applying the inverse Laplace transform to (54), the dynamic electric displacement intensity factor of the stationary crack in time domain is

$$K_{\mathrm{III}}^{(D),s}(t) = \frac{\varepsilon_{11} k_e^2}{e_{15}(1-k_e^2)} \sqrt{\frac{2}{\pi^3 h}} p \int_0^t Re\left[\frac{\sqrt{\tau - bh}}{\sqrt{t-\tau}(\tau - b_{\mathrm{bg}} h) Q_+(-\tau/h)} \right] \mathrm{d}\tau H(b_{\mathrm{bg}} h - t) + \frac{\varepsilon_{11} k_e^2 p}{e_{15}(1-k_e^2)} \sqrt{\frac{2}{\pi h}} H(t - b_{\mathrm{bg}} h). \tag{55}$$

In view of (55), it can be seen that the dynamic electric displacement intensity factor has similar characteristics to those of the dynamic stress intensity factor. Since both dynamic intensities jump to a constant value as the Bleustein–Gulyaev surface wave arrives at the crack tip, i.e. $t = b_{\mathrm{bg}} h$, it is assumed that the value exceeds its critical value and the crack starts to propagate with a constant velocity v along the line $y = 0$. The crack speed v is less than the surface wave speed, i.e. $v < c_{\mathrm{bg}}$. The applied symmetric concentrated loading p on the original crack faces represented in the moving coordinate system for $t > b_{\mathrm{bg}} h$ will have the following form

$$\tau_{yz}(\xi, 0, t) = -p\delta(\xi + v(t - b_{\mathrm{bg}} h) + h) H(t) \tag{56}$$

where $\xi = x - v(t - b_{\mathrm{bg}} h)$. Applying the Laplace transform to (56), the boundary condition expressed in the Laplace transform domain can be obtained as follows

$$\overline{\tau}_{yz}(\xi, 0, s) = \frac{1}{2\pi \mathrm{i}} \int_{\Gamma_\lambda} \frac{pd}{\lambda - d} \mathrm{e}^{sh(1 - b_{\mathrm{bg}} v)\lambda + s\lambda\xi} \mathrm{d}\lambda, \tag{57}$$

where $d = 1/v$ is the slowness of the crack speed. The applied traction on the crack faces, as expressed in (57), has the functional form $\mathrm{e}^{s\lambda\xi}$. Since the Laplace transform solutions of applying traction $\mathrm{e}^{s\eta\xi}$ on the crack faces have been solved in the previous section, the responses induced from the propagating crack tip can be constructed by superimposing the fundamental solutions in (47) and (48) and the stress distribution in (57). The results of dynamic intensities expressed in the Laplace transform will be

$$\overline{K}_{\mathrm{III}}^{(\tau),v}(s) = \frac{1}{2\pi \mathrm{i}} \int_{\Gamma_\lambda} \frac{pd\, \mathrm{e}^{sh(1 - b_{\mathrm{bg}} v)\lambda}}{\lambda - d} \left\{ -\frac{\sqrt{2} M_+^*(\lambda)}{\sqrt{s}} \right\} \mathrm{d}\lambda, \tag{58}$$

$$\overline{K}_{\mathrm{III}}^{(D),v}(s) = \frac{1}{2\pi \mathrm{i}} \int_{\Gamma_\lambda} \frac{pd\, \mathrm{e}^{sh(1 - b_{\mathrm{bg}} v)\lambda}}{\lambda - d} \left\{ -\frac{\varepsilon_{11} k_e^2 \sqrt{2} M_+^*(\lambda)}{e_{15}(\sqrt{1 - b^2 v^2} - k_e^2)\sqrt{s}} \right\} \mathrm{d}\lambda. \tag{59}$$

Inverting the Laplace transform of (58) and (59), the dynamic stress intensity factor and the dynamic electric displacement intensity factor for the propagating crack in time domain can be obtained as follows

$$K_{\mathrm{III}}^{(\tau),v}(t)=\frac{\sqrt{2(1-b_{\mathrm{bg}}v)h}p}{\sqrt{\pi^3(1-bv)}}\int_0^t Re\left[\frac{\sqrt{(1-bv)\tau-(1-b_{\mathrm{bg}}v)bh}}{\sqrt{t-\tau}(\tau-b_{\mathrm{bg}}h)\left[v\tau+(1-b_{\mathrm{bg}}v)h\right]Q_+^*\left(\frac{-\tau}{(1-b_{\mathrm{bg}}v)h}\right)}\right]\mathrm{d}\tau, \tag{60}$$

$$K_{\mathrm{III}}^{(D),v}(t)=\frac{\varepsilon_{11}k_e^2\sqrt{2(1-b_{\mathrm{bg}}v)h}p}{e_{15}(\sqrt{1-b^2v^2}-k_e^2)\sqrt{\pi^3(1-bv)}}\int_0^t Re\left[\frac{\sqrt{(1-bv)\tau-(1-b_{\mathrm{bg}}v)bh}}{\sqrt{t-\tau}(\tau-b_{\mathrm{bg}}h)\left[v\tau+(1-b_{\mathrm{bg}}v)h\right]Q_+^*\left(\frac{-\tau}{(1-b_{\mathrm{bg}}v)h}\right)}\right]\mathrm{d}\tau. \tag{61}$$

It is pointed out that the results in (60) and (61) are valid only for $t > b_{\mathrm{bg}}h$. By using contour integration, the integrals in (60) and (61) can be evaluated and yield

$$K_{\mathrm{III}}^{(\tau),v}(t)=\frac{(1-b_{\mathrm{bg}}v)p}{\sqrt{1-bv}Q_+^*(d)}\sqrt{\frac{2}{\pi[v(t-b_{\mathrm{bg}}h)+h]}}H(t-b_{\mathrm{bg}}h), \tag{62}$$

$$K_{\mathrm{III}}^{(D),v}(t)=\frac{\varepsilon_{11}k_e^2(1-b_{\mathrm{bg}}v)p}{e_{15}(\sqrt{1-b^2v^2}-k_e^2)\sqrt{1-bv}Q_+^*(d)}\sqrt{\frac{2}{\pi[v(t-b_{\mathrm{bg}}h)+h]}}H(t-b_{\mathrm{bg}}h). \tag{63}$$

The expression for $K_{\mathrm{III}}^{(\tau),v}(t)$ in (62) has the interesting form of the product of a function of the crack velocity $(1-b_{\mathrm{bg}}v)/(\sqrt{1-bv}Q_+^*(d))$ and the corresponding stationary crack solution $K_{\mathrm{III}}^{(\tau),s}(t)$ in (53) with a distance $v(t-b_{\mathrm{bg}}h)+h$ from the crack tip. The value $(1-b_{\mathrm{bg}}v)/(\sqrt{1-bv}Q_+^*(d))$ is a universal function that depends only on crack speed and piezoelectric material properties. Similarly, it is easy to find from (55) and (63) that the universal function for the dynamic electric displacement intensity factor is $(1-b_{\mathrm{bg}}v)(1-k_e^2)/[\sqrt{1-bv}(\sqrt{1-b^2v^2}-k_e^2)Q_+^*(d)]$. It can be verified that as the characteristic length $h\to 0$, the solutions in (62) and (63) are the same as the earlier results obtained in Li and Mataga (1996a). Furthermore, as the electro-mechanical coupling coefficient $k_e\to 0$, the solution expressed in (62) degenerates into the solution for anti-plane crack propagation in a purely elastic medium (Ma and Ing, 1997). If the crack speed $v\to 0$, (62) and (63) recover the solutions in (53) and (55).

It is worthy to note that the dynamic stress intensity factor $K_{\mathrm{III}}^{(\tau),v}(t)$ expressed in (62) goes to zero as v approaches c_{bg} for the particular electrode case. This agrees with the result in Li and Mataga (1996a). The vanishing of stress intensity factor at the Bleustein–Gulyaev surface wave speed provides the limiting speed for crack propagation. It is analogous to the case of in-plane crack extension for purely elastic materials, for which the limiting speed is the Rayleigh wave. The dynamic electric displacement intensity factor, however, does not vanish at the surface speed. With the aid of the identity

$$\sqrt{1-b^2v^2}-k_e^2=\frac{1-b_{\mathrm{bg}}v}{(1-k_e^4)(1+b_{\mathrm{bg}}v)(\sqrt{1-b^2v^2}+k_e^2)}, \tag{64}$$

the dynamic electric displacement intensity factor expressed in (63) attains the following finite non-zero value as v approaches c_{bg}

$$\lim_{v\to c_{\mathrm{bg}}}K_{\mathrm{III}}^{(D),v}(t)=\frac{\varepsilon_{11}k_e^2(1-k_e^4)(1+b_{\mathrm{bg}}v)(\sqrt{1-b^2v^2}+k_e^2)p}{e_{15}\sqrt{1-bv}Q_+^*(d)}\sqrt{\frac{2}{\pi[v(t-b_{\mathrm{bg}}h)+h]}}H(t-b_{\mathrm{bg}}h). \tag{65}$$

The energy release rate is another important quantity in dynamic fracture mechanics. As mentioned previously, there is no contribution from electric field to the dynamic energy release rate because of the special electrode boundary condition. The energy release rate can be calculated in a way similar to the purely elastic case and is computed by

$$G(t) \equiv 2\lim_{a\to 0}\int_{-a}^{a}\left[\tau_{yz}(\xi,0,t)\frac{\partial w}{\partial \xi}(\xi,0,t)+D_y(\xi,0,t)\frac{\partial \phi}{\partial \xi}(\xi,0,t)+vE\right]\mathrm{d}\xi$$
$$= 2\lim_{a\to 0}\int_{-a}^{a}\tau_{yz}(\xi,0,t)\frac{\partial w}{\partial \xi}(\xi,0,t)\,\mathrm{d}\xi. \tag{66}$$

To calculate the dynamic energy release rate, the shear stress τ_{yz} and anti-plane displacement w of the propagating crack along $y=0$ should be obtained first. Combining (57) with the fundamental solutions expressed in (41) and (44), the anti-plane displacement $\bar{w}$ and shear stress $\bar{\tau}_{yz}$ in the Laplace transform domain can be represented as follows

$$\overline{w}(\xi,y,s)=\frac{1}{2\pi \mathrm{i}}\int_{\Gamma_{\eta_1}}\frac{pd\,\mathrm{e}^{sh(1-b_{\mathrm{bg}}v)\eta_1}}{\eta_1-d}\mathrm{d}\eta_1\left\{\frac{-1}{2\pi \mathrm{i}}\int_{\Gamma_{\eta_2}}\frac{M_+^*(\eta_1)\sqrt{1/(c+v)-\eta_2}\,\mathrm{e}^{-s\alpha^*(\eta_2)y+s\eta_2\xi}}{\overline{c}_{44}(\sqrt{1-b^2v^2}-k_e^2)s(\eta_1-\eta_2)[1/(c_{\mathrm{bg}}+v)-\eta_2]Q_-^*(\eta_2)}\mathrm{d}\eta_2\right\}, \tag{67}$$

$$\overline{\tau}_{yz}(\xi,y,s)=\frac{1}{2\pi \mathrm{i}}\int_{\Gamma_{\eta_1}}\frac{pd\,\mathrm{e}^{sh(1-b_{\mathrm{bg}}v)\eta_1}}{\eta_1-d}\mathrm{d}\eta_1\left\{\frac{1}{2\pi \mathrm{i}}\int_{\Gamma_{\eta_2}}\frac{M_+^*(\eta_1)\alpha^*(\eta_2)\sqrt{1/(c+v)-\eta_2}\,\mathrm{e}^{-s\alpha^*(\eta_2)y+s\eta_2\xi}}{(\sqrt{1-b^2v^2}-k_e^2)(\eta_1-\eta_2)[1/(c_{\mathrm{bg}}+v)-\eta_2]Q_-^*(\eta_2)}d\eta_2\right.$$
$$\left.-\frac{1}{2\pi \mathrm{i}}\int_{\Gamma_{\eta_2}}\frac{k_e^2M_+^*(\eta_1)\alpha^*(\eta_2)\sqrt{1/(c+v)-\eta_2}\,\mathrm{e}^{-s\beta^*(\eta_2)y+s\eta_2\xi}}{(\sqrt{1-b^2v^2}-k_e^2)(\eta_1-\eta_2)[1/(c_{\mathrm{bg}}+v)-\eta_2]Q_-^*(\eta_2)}\mathrm{d}\eta_2\right\}. \tag{68}$$

By setting $y=0$, inverting the Laplace transform, and then taking the limit $x\to 0$, we can obtain

$$\lim_{\xi\to 0}\frac{\partial w}{\partial \xi}(\xi,0,t)$$
$$=\frac{\sqrt{(1-b_{\mathrm{bg}}v)h}p}{\pi^2\overline{c}_{44}(\sqrt{1-b^2v^2}-k_e^2)\sqrt{(1-bv)}}\lim_{\xi\to 0}\int_0^t Re\left[\frac{\sqrt{(1-bv)\tau-(1-b_{\mathrm{bg}}v)bh}H(-\xi)}{\sqrt{t-\tau}(\tau-b_{\mathrm{bg}}h)[v\tau+(1-b_{\mathrm{bg}}v)h]Q_+^*\left(\frac{-\tau}{(1-b_{\mathrm{bg}}v)h}\right)\sqrt{-\xi}}\right]\mathrm{d}\tau, \tag{69}$$

$$\lim_{\xi\to 0}\tau_{yz}(\xi,0,t)$$
$$=\frac{\sqrt{(1-b_{\mathrm{bg}}v)h}p}{\pi^2\sqrt{(1-bv)}}\lim_{\xi\to 0}\int_0^t Re\left[\frac{\sqrt{(1-bv)\tau-(1-b_{\mathrm{bg}}v)bh}H(\xi)}{\sqrt{t-\tau}(\tau-b_{\mathrm{bg}}h)[v\tau+(1-b_{\mathrm{bg}}v)h]Q_+^*\left(\frac{-\tau}{(1-b_{\mathrm{bg}}v)h}\right)\sqrt{\xi}}\right]\mathrm{d}\tau. \tag{70}$$

Substituting (69) and (70) into (66), and making use of the identity (Freund, 1972c)

$$\lim_{a\to 0}\int_{-a}^{a}\frac{H(\xi)}{\sqrt{\xi}}\frac{H(-\xi)}{\sqrt{-\xi}}\mathrm{d}\xi=\frac{\pi}{2} \tag{71}$$

the dynamic energy release rate of the propagating crack can be obtained as follows

$$G_v(t)=\frac{(1-b_{\mathrm{bg}}v)hp^2}{\pi^3\overline{c}_{44}(\sqrt{1-b^2v^2}-k_e^2)(1-bv)}\left\{\int_0^t Re\left[\frac{\sqrt{(1-bv)\tau-(1-b_{\mathrm{bg}}v)bh}}{\sqrt{t-\tau}(\tau-b_{\mathrm{bg}}h)[v\tau+(1-b_{\mathrm{bg}}v)h]Q_+^*\left(\frac{-\tau}{h(1-b_{\mathrm{bg}}v)}\right)}\right]\mathrm{d}\tau\right\}^2. \tag{72}$$

For time $t > b_{bg}h$, we can carry out the integral in (72) and have

$$G_v(t) = \frac{1}{2\overline{c}_{44}(\sqrt{1-b^2v^2}-k_e^2)}\left\{\frac{(1-b_{bg}v)p}{\sqrt{1-bvQ_+^*(d)}}\sqrt{\frac{2}{\pi[v(t-b_{bg}h)+h]}}\right\}^2 H(t-b_{bg}h)$$
$$= \frac{1}{2\overline{c}_{44}(\sqrt{1-b^2v^2}-k_e^2)}\left[K_{III}^{(\tau),v}(t)\right]^2. \tag{73}$$

Similar to the dynamic stress intensity factor, the dynamic energy release rate in (73) goes to zero as v approaches c_{bg}. Hence, we have not to study the supersonic case in this paper under the assumption of electrode boundary conditions.

Some special cases are examined here. By setting $v \to 0$, Eq. (72) can be reduced to the dynamic energy release rate of a stationary crack subjected to concentrated loading on the crack faces and yields

$$G_s(t) = \frac{p^2}{\pi^3 h\overline{c}_{44}(1-k_e^2)}\left\{\int_0^t Re\left[\frac{\sqrt{\tau-bh}}{\sqrt{t-\tau}(\tau-b_{bg}h)Q_+(-\tau/h)}\right]d\tau\right\}^2 = \frac{1}{2\overline{c}_{44}(1-k_e^2)}[K_{III}^{(\tau),s}(t)]^2. \tag{74}$$

As $h \to 0$, the expression in (73) is the same as the solution obtained in Li and Mataga (1996a). As $k_e \to 0$, Eq. (74) reduces to the well-known purely elastic results

$$G_s(t) = \frac{1}{2c_{44}}[K_{III}^{(\tau),s}(t)]^2. \tag{75}$$

4. Numerical results

In the previous section, the transient solutions for dynamic stress intensity factor, dynamic electric displacement intensity factor, and dynamic energy release rate of a propagating crack subjected to anti-plane concentrated loading on the crack faces are derived. In this section, numerical calculations are carried out to show the influence of the pertinent parameters. Three piezoelectric materials, $BaTiO_3$, PZT-4, and PZT-5, are chosen for numerical evaluations. The material properties of these three piezoelectric media are given in Table 1.

Fig. 2 shows the variation of the non-dimensional dynamic stress intensity factors with the normalized time t/bh for $v/c_{bg} = 0.3$. It can be seen that the stress intensity factors have no obvious difference for these three piezoelectric materials. Since the electrostatic potential is zero along the entire line $y = 0$, the transient response of the stationary crack keeps zero before the shear wave arrives at the crack tip ($t < bh$). Afterward it decreases violently during the stage $bh < t < b_{bg}h$, and reveals a singularity as the Bleustein–Gulyaev piezoelectric surface wave arrives at the crack tip ($t = b_{bg}h$). For time $t > b_{bg}h$, the crack starts to propagate and the dynamic stress intensity factor decreases smoothly from the static solution for the stationary crack. As indicated in (53), the static solution ($p\sqrt{2/(\pi h)}$) is independent of material properties.

The transient responses of the non-dimensional dynamic electric displacement intensity factors are shown in Fig. 3. The transient behavior is similar to that of dynamic stress intensity factor. However, it is

Table 1
Material properties of $BaTiO_3$, PZT-4, and PZT-5 piezoelectric media (Li and Mataga, 1996a)

Compound	$BaTiO_3$	PZT-4	PZT-5
ρ (kg/m^3)	5700	7500	7750
c_{44} (10^{10} N/m^2)	4.4	2.56	2.11
ε_{11} (10^{-10} C/Vm)	98.722	64.634	81.103
e_{15} (C/m^2)	11.4	12.7	12.3

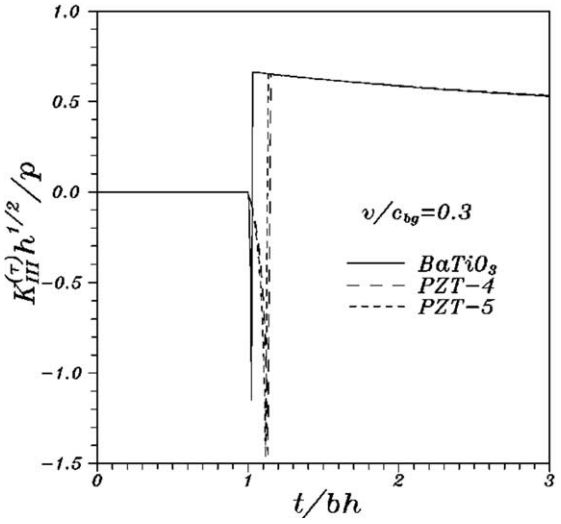

Fig. 2. Normalized dynamic stress intensity factors versus normalized time for various piezoelectric materials.

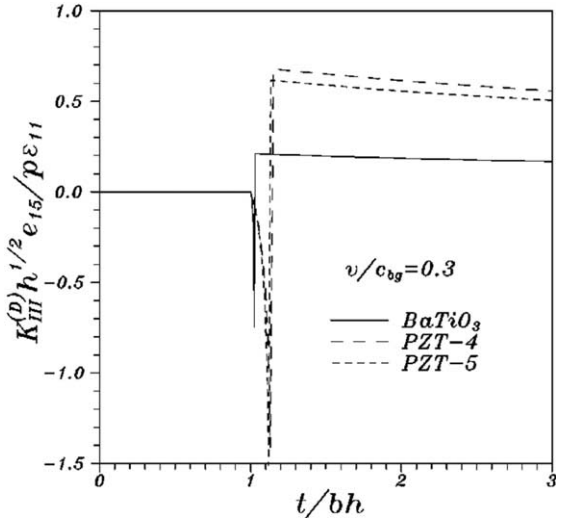

Fig. 3. Normalized dynamic electric displacement intensity factors versus normalized time for various piezoelectric materials.

pointed out that the jump values for static solutions are not the same as the surface wave passes the crack tip. Moreover, the dynamic electric displacement intensity factors exhibit apparent differences after the propagation of the crack for these three piezoelectric materials Fig. 4 shows the transient responses of the non-dimensional dynamic energy release rates. It can be seen that the magnitude of the dynamic energy release rate also approaches infinity as the surface wave reaches the crack tip, and then diminishes with time for $t > b_{bg}h$.

Figs. 5–7 show the dynamic stress intensity factor, the dynamic electric displacement intensity factor, and the dynamic energy release rate for different values of crack velocity v. It indicates that the stationary

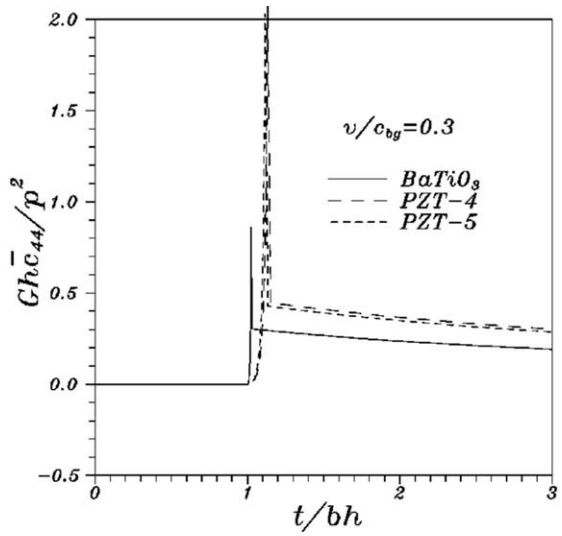

Fig. 4. Normalized dynamic energy release rates normalized time for various piezoelectric materials.

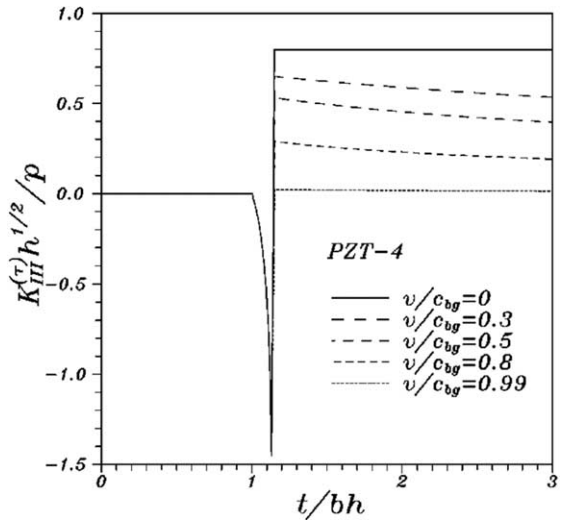

Fig. 5. Normalized dynamic stress intensity factors versus normalized time for different values of crack speed v.

crack will induce the largest dynamic intensity factors and energy release rate in all cases. In addition, the dynamic stress intensity factor and energy release rate are small when the magnitude of the ratio v/c_{bg} is large, while it is not always true for the dynamic electric displacement intensity factor. It can also be viewed that the dynamic stress intensity factor and energy release rate will go to zero as the propagating speed $v \to c_{\mathrm{bg}}$. However, the dynamic intensity factor for electric displacement does not vanish at the Bleustein–Gulyaev piezoelectric surface wave speed.

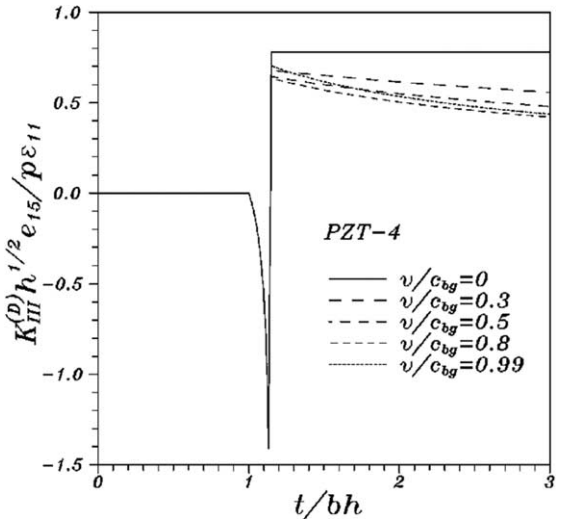

Fig. 6. Normalized dynamic electric displacement intensity factors versus normalized time for different values of crack speed v.

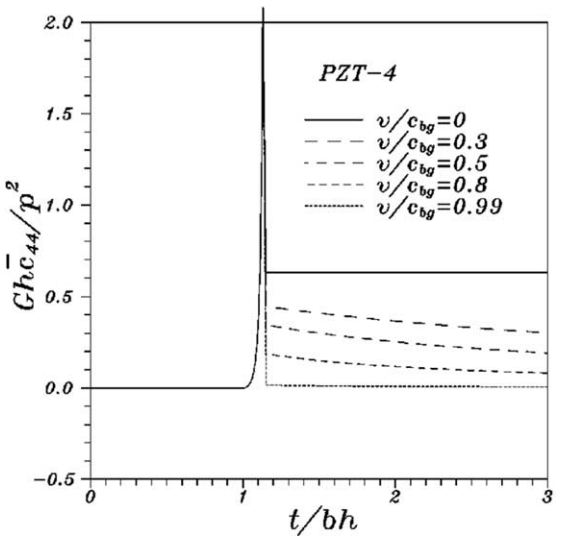

Fig. 7. Normalized dynamic energy release rates normalized time for different values of crack speed v.

5. Conclusions

The transient response of a propagating crack subjected to dynamic anti-plane concentrated loading in a piezoelectric medium has been investigated. It is assumed that the crack surfaces are coated with an infinitesimally thin conducting electrode that is grounded. A new fundamental solution for the piezoelectrically propagating crack is derived and the transient solutions are determined by superposition of the fundamental solution in the Laplace transform domain. Exact analytical transient solutions for the

dynamic stress intensity factor, the dynamic electric displacement intensity factor, and the dynamic energy release rate are obtained and expressed in explicit forms. It is found that the dynamic intensities and the dynamic energy release rate of a stationary crack will jump to the corresponding static values after the surface wave passes the crack tip. For the propagating case, the result indicates that the dynamic stress intensity factor and the dynamic energy release rate go to zero as the crack speed $v \to c_{bg}$. However, the dynamic intensity factor for electric displacement attains a non-zero value at the Bleustein–Gulyaev piezoelectric surface wave speed. The solution obtained in this paper can be considered to be a Green function for the associated problem. The solutions to problems of any arbitrary spatially distributed loading, or more general time dependence, can be obtained by superposition. Although only the intensities and energy release rate are derived in this study, the transient full-field solutions for the crack propagation problem can also be obtained by using the fundamental solutions proposed in Section 2.

Acknowledgements

The authors gratefully acknowledge the financial support of this research by the National Science Council (Republic of China) under Grant NSC 91-2212-E-032-002.

References

Achenbach, J.D., 1970a. Brittle and ductile extension of a finite crack by a horizontally polarized shear wave. International Journal of Engineering Science 8, 947–966.

Achenbach, J.D., 1970b. Extension of a crack by a shear wave. Zeitschrift fur Angewandte Mathematik und Physik (ZAMP) 21, 887–900.

Achenbach, J.D., 1973. Wave Propagation in Elastic Solids. Elsevier, New York.

Bleustein, J.L., 1968. A new surface wave in piezoelectric materials. Applied Physics Letters 13, 412–413.

Cagniard, L., 1939. Reflexion et Refraction des Ondes Seismiques Progressives. Gauthiers-Villars, Paris. Translated into English and revised by Flinn, E.A., Dix, C.H., 1962. Reflection and Refraction of Progressive Seismic Waves. McGraw-Hill, New York.

Chen, Z.T., 1998. Crack tip field of an infinite piezoelectric strip under anti-plane impact. Mechanics Research Communications 25, 313–319.

Chen, Z.T., Karihaloo, B.L., 1999. Dynamic response of a cracked piezoelectric ceramic under arbitrary electro-mechanical impact. International Journal of Solids and Structures 36, 5125–5133.

Chen, Z.T., Yu, S.W., 1997. Antiplane Yoffe crack problem in piezoelectric materials. International Journal of Fracture 84, L41–L45.

Chen, Z.T., Karihaloo, B.L., Yu, S.W., 1998. A Griffith crack moving along the interface of two dissimilar piezoelectric materials. International Journal of Fracture 91, 197–203.

Freund, L.B., 1972a. Crack propagation in an elastic solid subjected to general loading—I. Constant rate of extension. Journal of the Mechanics and Physics of Solids 20, 129–140.

Freund, L.B., 1972b. Crack propagation in an elastic solid subjected to general loading—II. Non-uniform rate of extension. Journal of the Mechanics and Physics of Solids 20, 141–152.

Freund, L.B., 1972c. Energy flux into the tip of an extending crack in an elastic solid. Journal of Elasticity 2, 341–349.

Freund, L.B., 1973. Crack propagation in an elastic solid subjected to general loading—III. Stress wave loading. Journal of the Mechanics and Physics of Solids 21, 47–61.

Freund, L.B., 1974. Crack propagation in an elastic solid subjected to general loading—IV. Obliquely incident stress pulse. Journal of the Mechanics and Physics of Solids 22, 137–146.

Gao, C.F., Fan, W.X., 1999a. A general solution for the plane problem in piezoelectric media with collinear cracks. International Journal of Engineering Science 37, 347–363.

Gao, C.F., Fan, W.X., 1999b. Exact solutions for the inplane problem in piezoelectric materials with an elliptic or a crack. International Journal of Solids and Structures 36, 2527–2540.

Gao, C.F., Wang, M.Z., 2001. Green's functions of an interfacial crack between two dissimilar piezoelectric media. International Journal of Solids and Structures 38, 5323–5334.

Ing, Y.S., Lin, J.T., 2002. Dynamic full-field analysis of a surface crack subjected to an antiplane moving loading. Journal of the Chinese Institute of Engineers 25, 639–651.

Ing, Y.S., Ma, C.C., 1996. Transient response of a finite crack subjected to dynamic antiplane loading. International Journal of Fracture 82, 345–362.
Ing, Y.S., Ma, C.C., 1997a. Dynamic fracture analysis of a finite crack subjected to an incident horizontally polarized shear wave. International Journal of Solids and Structures 34, 895–910.
Ing, Y.S., Ma, C.C., 1997b. Transient analysis of a subsonic propagating interface crack subjected to anti-plane dynamic loading in dissimilar isotropic materials. Journal of Applied Mechanics 64, 546–556.
Ing, Y.S., Ma, C.C., 1999. Transient analysis of a propagating crack with finite length subjected to a horizontally polarized shear wave. International Journal of Solids and Structures 36, 4609–4627.
Ing, Y.S., Ma, C.C., 2001. Transient response of a surface crack subjected to dynamic anti-plane concentrated loadings. International Journal of Fracture 109, 239–261.
Ing, Y.S., Ma, C.C., 2003. Dynamic fracture analysis of finite cracks by horizontally polarized shear waves in anisotropic solids. Journal of the Mechanics and Physics of Solids 51, 1987–2021.
Ing, Y.S., Ma, C.C., submitted for publication. Full-field analysis of an anisotropic finite crack subjected to an anti-plane point impact loading.
Ing, Y.S., Wang, M.J., 2004. Explicit transient solutions for a mode III crack subjected to dynamic concentrated loading in a piezoelectric material. International Journal of Solids and Structures 41, 3849–3864.
Kostrov, B.V., 1964. Self-similar problems of propagation of shear cracks. Applied Mathematics and Mechanics (PMM) 28, 1077–1087.
Kostrov, B.V., 1966. Unsteady propagation of longitudinal shear cracks. Prikladnaya Matematika I Mekhanika 30, 1241–1248.
Kwon, S.M., Lee, K.Y., 2000. Analysis of stress and electric field in a rectangular piezoelectric body with a center crack under anti-plane shear loading. International Journal of Solids and Structures 37, 4859–4869.
Kwon, S.M., Lee, K.Y., 2001. Transient response of a rectangular piezoelectric medium with a center crack. European Journal of Mechanics A/Solids 20, 457–468.
Kwon, J.H., Lee, K.Y., Kwon, S.M., 2000. Moving crack in a piezoelectric ceramic strip under anti-plane shear loading. Mechanics Research Communications 27, 327–332.
Li, S., 2003. On global energy release rate of a permeable crack in a piezoelectric ceramic. Journal of Applied Mechanics 70, 246–252.
Li, S., Mataga, P.A., 1996a. Dynamic crack propagation in piezoelectric materials—Part I. Electrode solution. Journal of the Mechanics and Physics of Solids 44, 1799–1830.
Li, S., Mataga, P.A., 1996b. Dynamic crack propagation in piezoelectric materials—Part II. Vacuum solution. Journal of the Mechanics and Physics of Solids 44, 1831–1866.
Li, X.F., 2001. Transient response of a piezoelectric material with a semi-infinite mode-III crack under impact loads. International Journal of Fracture 111, 119–130.
Ma, C.C., 1988. Initiation, propagation, and kinking of an in-plane crack. Journal of Applied Mechanics 55, 587–595.
Ma, C.C., 1990. Dynamic mixed mode I–II crack kinking under oblique stress wave loading in brittle solids. Journal of Applied Mechanics 57, 117–127.
Ma, C.C., Burgers, P., 1986. Mode III kinking with delay time: an analytical approximation. International Journal of Solids and Structures 22, 883–899.
Ma, C.C., Burgers, P., 1987. Dynamic mode I and mode II crack kinking including delay time effects. International Journal of Solids and Structures 23, 897–918.
Ma, C.C., Burgers, P., 1988. Initiation, propagation, and kinking of an antiplane crack. Journal of Applied Mechanics 55, 111–119.
Ma, C.C., Ing, Y.S., 1997. Dynamic crack propagation in a layered medium under antiplane shear. Journal of Applied Mechanics 64, 66–72.
Meguid, S.A., Chen, Z.T., 2001. Transient response of a finite piezoelectric strip containing coplanar insulating cracks under electromechanical impact. Mechanics of Materials 33, 85–96.
Meguid, S.A., Zhao, X., 2002. The interface crack problem of bonded piezoelectric and elastic half-space under transient electromechanical loads. Journal of Applied Mechanics 69, 244–253.
Narita, F., Shindo, Y., 1998a. Layered piezoelectric medium with interface crack under anti-plane shear. Theoretical and Applied Fracture Mechanics 30, 119–126.
Narita, F., Shindo, Y., 1998b. Dynamic anti-plane shear of a cracked piezoelectric ceramic. Theoretical and Applied Fracture Mechanics 29, 169–180.
Narita, F., Shindo, Y., 1999. Scattering of antiplane shear waves by a finite crack in piezoelectric laminates. Acta Mechanica 134, 27–43.
Pak, Y.E., 1990. Crack extension force in a piezoelectric material. Journal of Applied Mechanics 57, 647–653.
Park, S.B., Sun, C.T., 1995a. Effect of electric field on fracture of piezoelectric ceramics. International Journal of Fracture 70, 203–216.
Park, S.B., Sun, C.T., 1995b. Fracture criteria of piezoelectric ceramics. Journal of the American Ceramic Society 78, 1475–1480.
Qin, Q.H., Mai, Y.W., 1998. Multiple cracks in thermoelectroelastic bimaterials. Theoretical and Applied Fracture Mechanics 29, 141–150.

Ru, C.Q., 2000. Exact solution for finite electrode layers embedded at the interface of two piezoelectric half-planes. Journal of Mechanics and Physics of Solids 48, 693–708.

Shen, S., Kuang, Z.B., Hu, S., 1999. Interface crack problems of a laminated piezoelectric plate. European Journal of Mechanics A/Solids 18, 219–238.

Shin, J.W., Kwon, S.M., Lee, K.Y., 2001. An eccentric crack in a piezoelectric strip under anti-plane shear impact loading. International Journal of Solids and Structures 38, 1483–1494.

Shindo, Y., Ozawa, E., 1990. Dynamic analysis of a piezoelectric material. In: Hsieh, R.K.T. (Ed.), Mechanical Modeling of New Electromagnetic Materials. Elsevier, Amsterdam, pp. 297–304.

Sosa, H., 1992. On the fracture mechanics of piezoelectric solids. International Journal of Solids and Structures 29, 2613–2622.

Suo, Z., Kuo, C.M., Barnett, D.M., Willis, J.R., 1992. Fracture mechanics of piezoelectric ceramics. Journal of the Mechanics and Physics of Solids 40, 739–765.

Ueda, S., 2003. Diffraction of antiplane shear waves in a piezoelectric laminate with a vertical crack. European Journal of Mechanics A/Solids 22, 413–422.

Wang, B.L., Han, J.C., Du, S.Y., 2000. Electroelastic fracture dynamics for multilayered piezoelectric materials under dynamic anti-plane shearing. International Journal of Solids and Structures 37, 5219–5231.

Wang, X.D., 2001. On the dynamic behaviour of interacting interfacial cracks in piezoelectric media. International Journal of Solids and Structures 38, 815–831.

Wang, X.D., Meguid, S.A., 2000. Modelling and analysis of the dynamic behaviour of piezoelectric materials containing interacting cracks. Mechanics of Materials 32, 723–737.

Yang, F., 2001. Fracture mechanics for a mode I crack in piezoelectric materials. International Journal of Solids and Structures 38, 3813–3830.

Yang, F., Kao, I., 1999. Crack problem in piezoelectric materials: general anti-plane mechanical loading. Mechanics of Materials 31, 395–406.

Yoffe, E.H., 1951. The moving Griffith crack. Philosophical Magazine 42, 739–750.

Zhang, T.Y., Tong, P., 1996. Fracture mechanics for mode III crack in a piezoelectric material. International Journal of Solids and Structures 33, 343–359.

Zhao, X., Meguid, S.A., 2002. On the dynamic behaviour of a piezoelectric laminate with multiple interfacial collinear cracks. International Journal of Solids and Structures 39, 2477–2494.

Zhou, Z.G., Wang, B., Sun, Y.G., 2003. Investigation of the dynamic behavior of two parallel symmetric cracks in piezoelectric materials use of non-local theory. International Journal of Solids and Structures 40, 747–762.